Article

Journal of
Nanoscience and Nanotechnology
Vol. 16, 2474–2481, 2016
www.aspbs.com/jnn

Size-Dependent Biodistribution of Iodinated Oil Nanoemulsions Observed by Dual-Modal Imaging in Rats

Gong Chen[1,2], Ziyu He[2], Xiaoli Yu[2], Ting Wang[2], Chengkai Gao[1], Lina Song[1], Haoan Wu[1], Changjun Yin[2], Shouhua Luo[1], Yu Zhang[1,*], and Ning Gu[1,*]

[1]*State Key Laboratory of Bioelectronics, Jiangsu Key Laboratory for Biomaterials and Devices, School of Biological Science and Medical Engineering and Collaborative Innovation Center of Suzhou Nano Science and Technology, Southeast University, Nanjing 210096, P. R. China*
[2]*Affiliated Hospital of Nanjing University of Traditional Chinese Medicine, Nanjing 210029, P. R. China*

Sizes of nanoscale contrast agents play an important role in targeting specific organs and distribution in organisms. Iodinated oil nanoemulsions with uniform size distribution and containing indocyanine green (ICG) fluorescent dye (25 nm, 60 nm, 100 nm) were synthesized by stirring, combined with ultrasonic emulsification technique. Rats were intravenously injected with the iodinated oil nanoemulsions with different sizes, used as contrast agents, and investigated with enhanced computed tomography (CT) and fluorescence imaging. Through experiments, the distribution and metabolism of the contrast agents in rat's bodies were studied, and their influence on enhanced CT imaging of different organs was compared. The results demonstrated that target accumulating organs for the iodinated oil nanoemulsions were liver and spleen, with obvious dosage-dependence. Large sized nanoemulsion preferred to accumulate into spleen, and liver, and the phagocytosis was getting weaker with the decrease of the nanoemulsion size. The CT imaging of the inferior vena cava was rapidly enhanced and reached the highest point after administration of the nanoemulsion. The nanoemulsion gradually gathered and metabolized in the spleen and liver, resulting in rapidly decreased CT imaging, with weak rebound, of the inferior vena cava.

Keywords: Iodinated Oil, Nanoemulsions, Dual-Modal Imaging, Rat.

1. INTRODUCTION

The currently most common imaging diagnostic methods at home and abroad include X-ray computed tomography (CT), magnetic resonance imaging (MRI), positron emission tomography (PET), fluorescence imaging and ultrasound imaging. Due to different imaging principles, the diagnostic imaging methods have different imaging features and advantages and disadvantages. Because each imaging method has relatively independent examination results, it is not able to get complete body's internal biological information for complex diseases using a single imaging technique.

Molecularimaging (MI) utilizes the existing imaging techniques to do real-time noninvasive imaging of specific molecules in biological processes in living tissues and at cellular and molecular levels. It shows molecular changes in living conditions and makes qualitative and quantitative description in research.[1–4] With development of MI, multimodal contrast probes appear at the same moment. Multimodal contrast agents are made up of a combination of traditional medical imaging techniques and molecular biology techniques. Compared with ordinary contrast agents, they can be used in multimodal imaging technique and are non-invasive, capable of detection at protein and nucleic acids molecular level, with high sensitivity.[5–8] Using multimodal contrast agents can not only get diagnosis in different imaging modes in one time medication, but also reduce the side effects from the drug, and also reduce the suffering of patients to achieve a multiplier effect.

Nanomaterials have a profound impact on clinical diagnosis and treatment, especially some new nanometer-sized contrast agents that can accurately locate lesions and image them at molecular level.[9–17] Nanoemulsion, also known as microemulsion with 10–100 nm diameters, is a thermodynamic stable system which is synthesized by water, oil, surfactants and co-surfactants in

*Authors to whom correspondence should be addressed.

 1533-4880/2016/16/2474/008 doi:10.1166/jnn.2016.12546

certain proportion. Emulsion droplets are mostly spherical liquid with uniform size and transparent or translucent appearance.[18–22] Nanoemulsion is a popular new drug delivery system in recent years. Jarzyna et al.,[23] Gianella et al.[24] and Wang et al.[25] have all created dual-modal contrast agents by using nanoemulsions.

Fluorescent imaging is very sensitive and combines the fluorescent probes to image molecules in the target organs. However, the low penetration and resolution limit its wide application inside the organs. CT is one of the most widely used diagnostic tools due to different X-ray absorption in tissues and lesions. This is a high-resolution imaging technology. Clinical contrast agents for the CT contrast enhancement are based on iodinated molecules and compounds with high X-ray absorption coefficient.[26–31] Liu[32] used the indocyanine green (ICG) fluorescent dye and iodinated oil as raw materials to prepare CT/fluorescent dual-modal ICG-Der-01-iodinated oil nanoemulsions. However, metabolism and imaging of the contrast agents in small animals were not studied. This current study prepared dual-modal ICG-Der-01-iodinated oil nanoemulsions with 3 different sizes: 25 nm, 60 nm and 100 nm. We analyzed distribution and metabolism of the contrast agents in rat's body by observing the enhanced CT images of multiple organs in the rats, using the synthesized nanoemulsion as contrast agent. This study also discusses how the injected volume of iodized oil nanoemulsion and hydrodynamic size of the contrast agents affected the enhanced CT images from the rats, and discovered the metabolic rule of different hydrodynamic size of the contrast agents in rats.

2. MATERIALS AND METHODS

2.1. Materials

Iodinated oil injection (Guerbet, France), ICG-Der-01 (China Pharmaceutical University), Lecithin (Lipoid, German), Polyoxyethylene glycol monostearate (25) (Jing Chun Industrial Co., Ltd. Shanghai, China), Phosphotungstic acid (Sinopharm Chemical Reagent Co., Ltd.), Ethanol (Sinopharm Chemical Reagent Co., Ltd.), Chloroform (Shanghai Chemical Co. Shenbo). Kunming female mice, sd female rat; 10% chloral hydrate.

Clinical CT (Brilliance 64 Channel, Philips, Holland); Fluorescence Imaging System (Maestro 2.10.0, CRI); Instrument: KQ-500DE ultrasonic cleaner (Kunshan Ultrasonic Instrument Co., Ltd.), DHG-9078A Electric vacuum drying oven (Shanghai Jing Hong Experimental Equipment Co., Ltd.), JJ-1 Precision force electric mixer (Guohua Electric Co., Ltd.), DF-101S Collector-type thermostat heating magnetic stirrer (Yu Hua Instrument Co. Gongyi City), Nano-ZS90 Dynamic light scattering instrument (DLS, Malvern Instruments Ltd., Britain), JEM-200CX Transmission electron microscopy (TEM, JEOL company, Japan), JY92-IIN Ultrasonic cell grinder (Xin Chi Biotechnology Co., Ltd. Ningbo), CP114 Electronic analytical balance (Ohaus Instrument Co., Ltd.), EDI-1001-U Water Purifier (Yi-yang Enterprise Development Corporation Chongqing).

2.2. Methods

2.2.1. Preparation of the ICG-Der-01 Fluorescent Dye-Iodine Oil Nanoemulsion

We used Iodinated oil injection as CT contrast agents and oil soluble ICG-Der-01 fluorescent dye as near-infrared fluorescent probes. The ICG-Der-01 fluorescent dye-iodine oil nanoemulsion was prepared, under the effect of mixed emulsifier PEG(25) monostearate and lecithin, by ultrasound after stirring. Briefly, 0.5 mg of ICG-Der-01 fluorescent dye (emission wavelength 805 nm) was dissolved into 1 mL chloroform solution. The solution was sonicated by ultrasonic cleaner for 10 min after a few seconds with effect from the concussion instrument, to ensure that the fluorescent dye completely dissolved in chloroform. 500 μL of Iodinated oil injection was then added into the above solution. The mixed solution was then put in ultrasonic cleaner for 5 min and served as oil phase. A certain amount of Lipoid E-80 was dissolved in ethanol and Polyoxyethylene glycol monostearate was dissolved in 30 mL of ultra-pure water in three-necked flask. The three-necked flask was placed on thermostat heating magnetic stirrer and heated to boiling water phase. The Lipoid E-80, ICG-Der-01 fluorescent dye and iodized oil injection which made up the oil phase were added drop wise into the boiling water which served as water phase. After mechanical stirring for 30 min, crude emulsion was prepared. The crude emulsion was then cooled to room temperature and diluted to 10 mL. Subsequently, the crude emulsion was sonicated under probe ultrasonication for 15 min (pulse: 2 s/3 s; 650 W, 20 kHz) and thereafter filtered by 220 nm membrane filter. The final nanoemulsion was stored in the dark at 4 °C.

Formulation of the small nanoemulsion involved: 350 mg PEG(25) Polyoxyethylene glycol monostearate, 200 mg Lipoid E-80, 1 mL Iodinated oil injection, and 50% ultrasonic power.

Formulation of the medium nanoemulsion involved: 200 mg PEG(25) Polyoxyethylene glycol monostearate, 100 mg Lipoid E-80, 1 mL Iodinated oil injection, 30% ultrasonic power.

Formulation of the large nanoemulsion involved: 200 mg PEG(25) Polyoxyethylene glycol monostearate, 100 mg Lipoid E-80, 2 mL Iodinated oil injection, and 30% ultrasonic power.

2.2.2. In Vivo Fluorescence Imaging

We performed the *ex vivo* fluorescence imaging to investigate the *in vivo* distribution of the median sized (60 nm) ICG-Der-01-iodinated oil nanoemulsion in mouse. After pre-scans, the mouse was tail vein injected with 200 μL of nanoemulsion and scanned at several time points postinjection (10 min, 30 min, 60 min, 90 min, and 120 min).

Table I. Details of iodinated oil nanoemulsions used as CT imaging contrast agent.

	Iodine (mg/mL)	Injection dosage (mL)	Size (nm)
Rat 1	48	2.5	60
Rat 2	48	2.0	100
Rat 3	48	2.0	60
Rat 4	48	1.0	60
Rat 5	48	2.0	25

2.2.3. *In Vivo* CT Imaging

5 sd rats were weighted and anaesthetized by 10% chloral hydrate (3 mL/KG body weight) via stomach. The 5 rats were then scanned by a clinical CT (Brilliance 64 Channel, Philips, Holland). All scans were accomplished with following parameters: tube voltage, 80 kV; current intensity, 250 mAs; slice thickness, 1 mm; pitch, 0.797. The concentrations, dosages and sized of the ICG-Der-01-iodinated oil nanoemulsion injected into the 5 rats are listed in the Table I.

After intravenous nanoemulsion, injection 5 rats were scanned at several time points post injection (at 1 min, 3 min, 5 min, 10 min, 20 min, 80 min, 140 min, and 200 min). All scans were accomplished with following parameters: tube voltage, 80 kV; current intensity, 250 mAs; slice thickness, 1 mm; pitch, 0.797.

2.2.4. Interest Area Selection and Measurement

5 rats were scanned at 9 time points (that is 0 min, 1 min, 3 min, 5 min, 10 min, 20 min, 80 min, 140 min, and 200 min). The window width was 600 and window level was 50. The selected interest area was used to measure the CT values in triplicate. The interest areas were as follows: two cortexes near the heart and liver respectively in the inferior vena cava with 1 mm^2 area; three parts near the subxyphoid edge in the lobe of the liver with 3 mm^2 area; and three parts near the costal margin in the spleen with of 1–2 mm^2 area.

3. RESULTS AND DISCUSSION

3.1. Morphology of the ICG-Der-01 Fluorescent Dye-Iodine Oil Nanoemulsion

DLS and TEM were used to characterize the hydrodynamic size and morphology of the synthesized ICG-Der-01 fluorescent dye-iodine oil nanoemulsion (shown in Fig. 1). The hydrodynamic sizes of the nanoemulsion were 25 nm, 60 nm and 100 nm, respectively. The TEM image showed that the nanoemulsion had a spherical shape with consistent size distribution compared with the DLS results.

3.2. *In Vivo* Fluorescence Imaging

Fluorescence imaging was used to investigate the *in vivo* distribution of the fluorescence dye-iodinated oil nanoemulsion in mouse. After pre-scans, the mouse was intravenously injected with the nanoemulsion and scanned at several time points after injection (10 min, 30 min, 60 min, 90 min, and 120 min). The change of distribution in mouse is shown in Figure 2. 10 min after tail vein injection, the dual-modal nanoemulsion was rapidly around the body. The nanoemulsion began to gather in the liver rather than other organs as time went by, indicating that the prepared fluorescent dye-iodinated oil nanoemulsion had high liver targeting. Further information could not be provided due to limitations from low resolution and tissue penetration depths of the fluorescent imaging.

3.3. CT Imaging Results

After intravenous injection with the nanoemulsion, 5 rats were scanned at several time points post injection. All scans

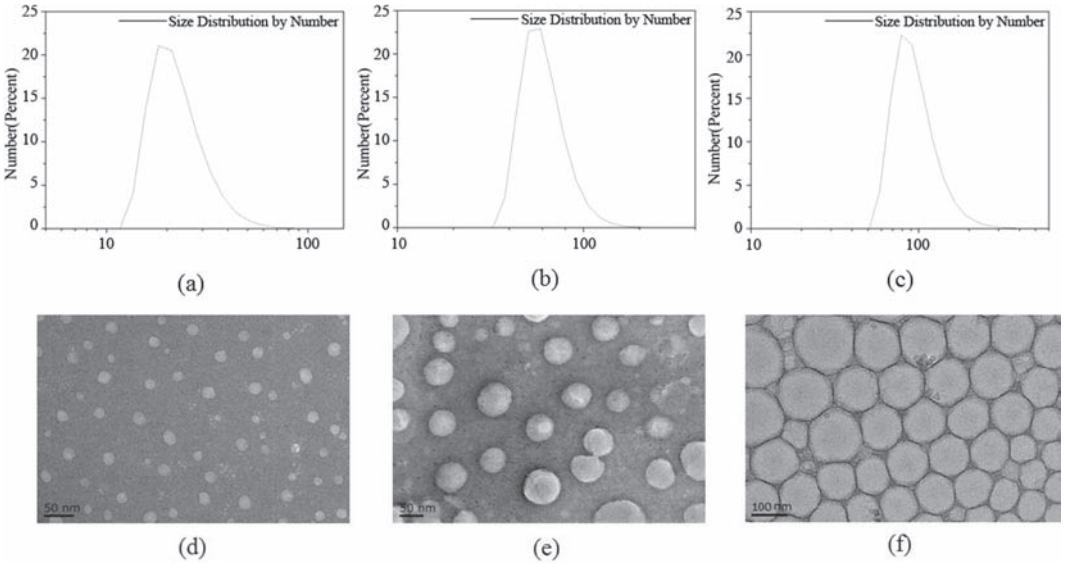

Figure 1. DLS and TEM images of three nanosized iodinated oil nanoemulsions, (a, d) 25 nm, (b, e) 60 nm and (c, f) 100 nm.

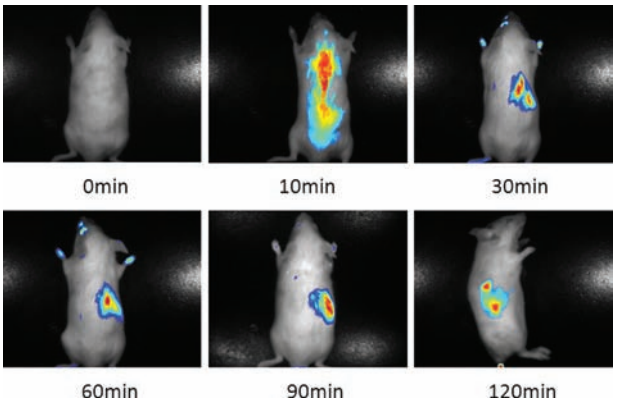

Figure 2. Distribution of fluorescence dye-iodinated oil nanoemulsions in mouse.

were accomplished with following parameters: tube voltage, 80 kV; current intensity, 250 mAs; slice thickness, 1 mm; pitch, and 0.797. Figure 3 illustrates the plain CT scan and enhanced scan images from the heart (a) (d), liver (b) (e) and spleen (c) (f) 1 min–5 min after administration into rat 2. The uniformed enhanced efficacy was clearly observed in the aortic lumen. Figure 4 illustrates the 3D reconstructed image of rat 2 at 1 min. The aorta of rat 2 was significantly enhanced as shown in Figure 4.

3.4. Size-Dependent Distribution of Iodinated Oil Nanoemulsion via CT

3.4.1. Inferior Vena Cava

5 rats were injected with different sizes of nanoemulsion and the CT values in the inferior vena cava are shown in Table II. The changes of CT values in the inferior vena cava 200 min after administration are shown in Figure 5(a). 1 min after administration, the CT values from the inferior vena cava rapidly reached the top in Rat 2, 3 and 5, suggesting that the nanoemulsion with different sizes (25 nm, 60 nm and 100 nm) could arrive at the heart within 1 min. The CT values decreased and the peak disappeared after 5 min. The iodine oil nanoemulsion was metabolized by the liver and spleen as time went by, meaning that the iodinated oil was slowly released to the blood, and the CT imaging from the inferior vena cava was enhanced again, getting to the highest point at around 80 min. The concentration of iodinated oil decreased to a stable value after 80 min. In comparison with the small sized nanoemulsion, the CT imaging was greatly enhanced by the large sized nanoemulsion with higher first peak and delayed second peak. The reason may be that the liver and spleen were had difficulty metabolizing large sized nanoemulsion, hence the iodinated oil was lately released to the blood.

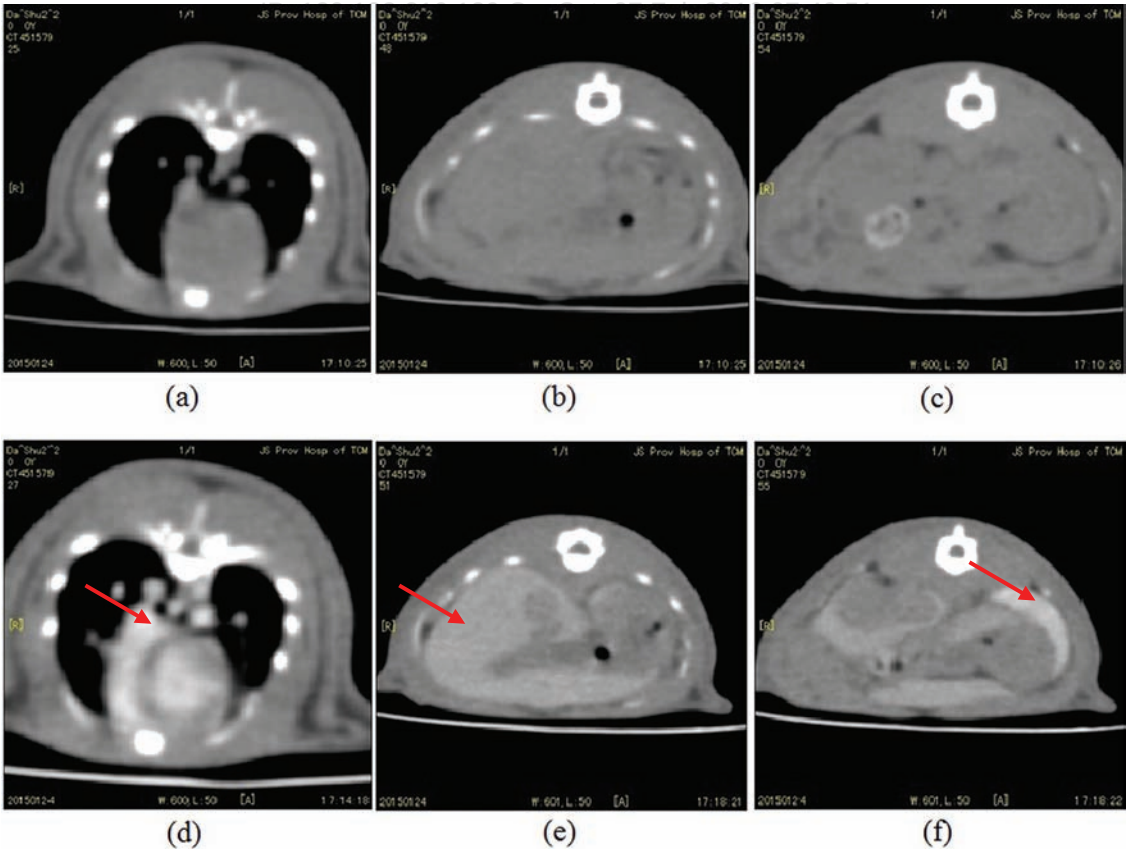

Figure 3. CT images for plain scan and enhanced scan in the rat 2, (a, d) heart, (b, e) liver and (c, f) spleen.

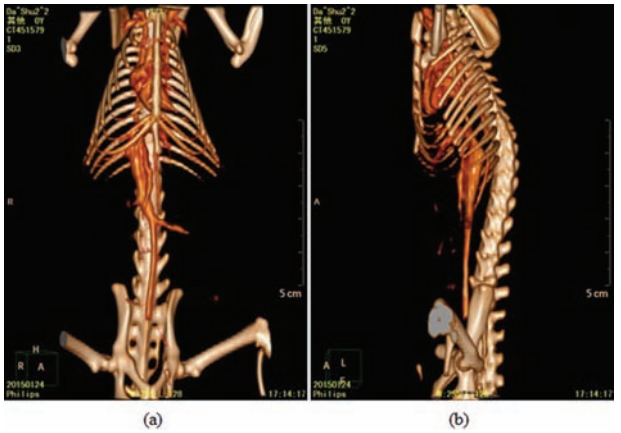

Figure 4. 3D reconstructed images of rat 2, (a) coronal and (b) sagittal.

A slightly higher dosage of nanoemulsion in rat 3 was administrated into rat 1. However, the CT value from the inferior vena cava in Rat 1 did not reach the top within 1 min. This was probably due to the short retention time of contrast agent in the inferior vena cava and differences between rats, causing a transient peak loss. Obvious peak was not observed in rat 4, this being probably caused by similar reason and low dosage of administrated nanoemulsion. The changes of CT values in rat 1, 3 and 4 suggested that if the nanoemulsion was at the same concentration (48 mg·I/mL) and size (60 nm), the less dosage (2.5, 2 and 1 mL) led to weaker CT efficacy and smaller CT values from the inferior vena cava imaging.

3.4.2. Liver

5 rats were injected with different sizes of nanoemulsion and CT values from the liver are shown in Table III. The changes of CT values in the liver 200 min after administration are shown in Figure 5(b). The CT values from the liver were substantially enhanced and reached a short stable stage after 5 min after administration. The contrast agent accumulated in the liver after 20 min, and the values reached the top at around 100 min. The CT imaging was also consistent with the fluorescence imaging. Moreover, the nanoemulsions with different sizes of 100 nm, 60 nm and 25 nm were administrated into rat 2, 3 and 5, respectively. Specifically, the 60 nm nanoemulsion gathered in liver mostly, followed by the 100 nm nanoemulsion. The 25 nm nanoemulsion gathered lastly in the liver, the possible reason being that most of the 100 nm nanoemulsion had accumulated in the spleen (Fig. 5(c)).

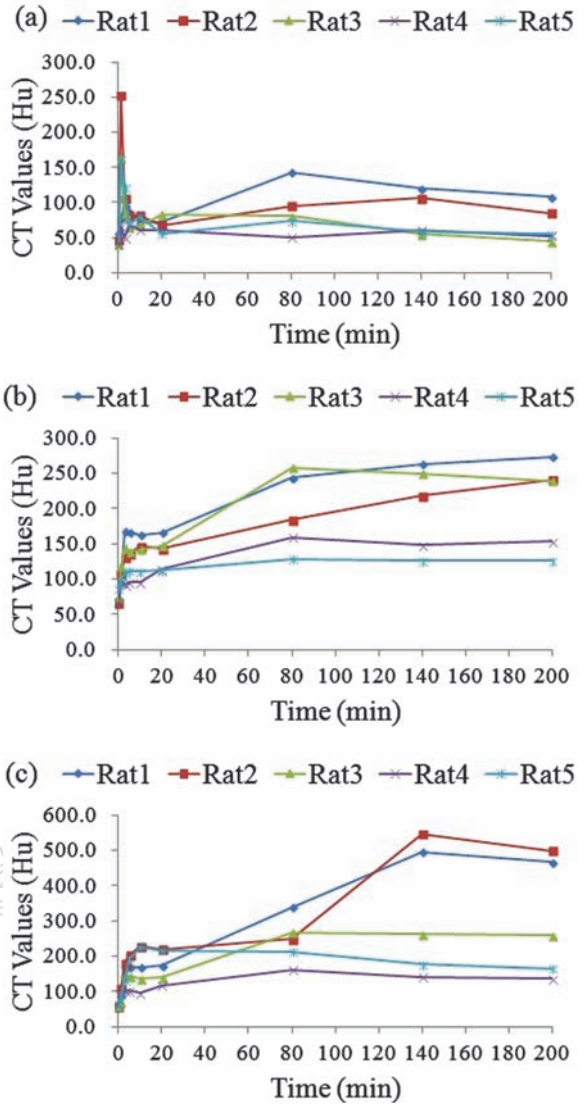

Figure 5. Plots of CT values with time in the organs of rats, (a) inferior vena cava, (b) liver and (c) spleen.

Table II. CT values in the inferior vena cava.

Time (min)	Rat 1 (Hu)	Rat 2 (Hu)	Rat 3 (Hu)	Rat 4 (Hu)	Rat 5 (Hu)
0	56	46	40	40	51
1	76.5	252	163.5	65.5	162
3	96	105	85	49.5	121
5	88	80.5	65.5	67	71
10	71	80.5	68	60	80
20	72	67.5	83.5	60.5	56
80	143	95	81	50.5	74
140	120	106	55	60.5	58
200	108.5	85	44.5	52.5	54.5

Table III. CT values in the liver.

Time (min)	Rat 1 (Hu)	Rat 2 (Hu)	Rat 3 (Hu)	Rat 4 (Hu)	Rat 5 (Hu)
0	73.0	65.7	73.7	66.3	86.7
1	95.7	109.3	118.3	94.3	97.7
3	168.7	131.7	145.0	92.0	109.0
5	167.3	136.3	138.7	95.3	111.7
10	162.7	146.7	142.3	95.3	111.0
20	166.0	143.3	147.3	114.0	113.0
80	244.0	184.7	257.7	159.0	128.7
140	263.7	218.3	250.0	148.3	126.3
200	273.3	241.0	239.7	153.0	126.3

Table IV. CT values in the spleen.

Time (min)	Rat 1 (Hu)	Rat 2 (Hu)	Rat 3 (Hu)	Rat 4 (Hu)	Rat 5 (Hu)
0	60.7	56.7	59.0	63.7	57.7
1	88.0	108.7	69.7	96.7	89.3
3	164.7	180.7	144.3	100.0	132.0
5	169.7	203.0	142.7	103.0	191.3
10	169.3	229.7	136.0	95.7	225.3
20	173.0	220.3	140.0	117.0	215.3
80	339.0	249.7	266.3	161.7	213.7
140	495.0	547.3	262.3	141.7	177.0
200	467.7	500.0	259.0	135.7	163.7

The size of the nanoemulsion injected into rat 2 was 100 nm. The larger the nanoemulsion was, the more slowly it was metabolized by the liver and therefore the large sized nanoemulsion more slowly gathered into the liver and its peak value appeared lately. The size of the nanoemulsion injected into rat 5 was 25 nm. The enhanced efficacy of the small sized nanoemulsion was obviously weaker than the larger sized nanoemulsion and therefore although the small sized nanoemulsion was metabolized quickly by the liver, their enhanced efficacy was not as strong as that of the larger sized nanoemulsion. The changes of CT values in rat 1, 3 and 4 suggested that if the nanoemulsion was at the same concentration (48 mg · I/mL) and size (60 nm), the less dosage led to weaker CT efficacy and smaller CT value in the liver.

3.4.3. Spleen

5 rats were injected with different sizes of nanoemulsion and the CT values from the spleen are shown in Table IV. The changes of CT values in the spleen 200 min after administration are shown in Figure 5(c). The CT values from the spleen were substantially enhanced and reached a

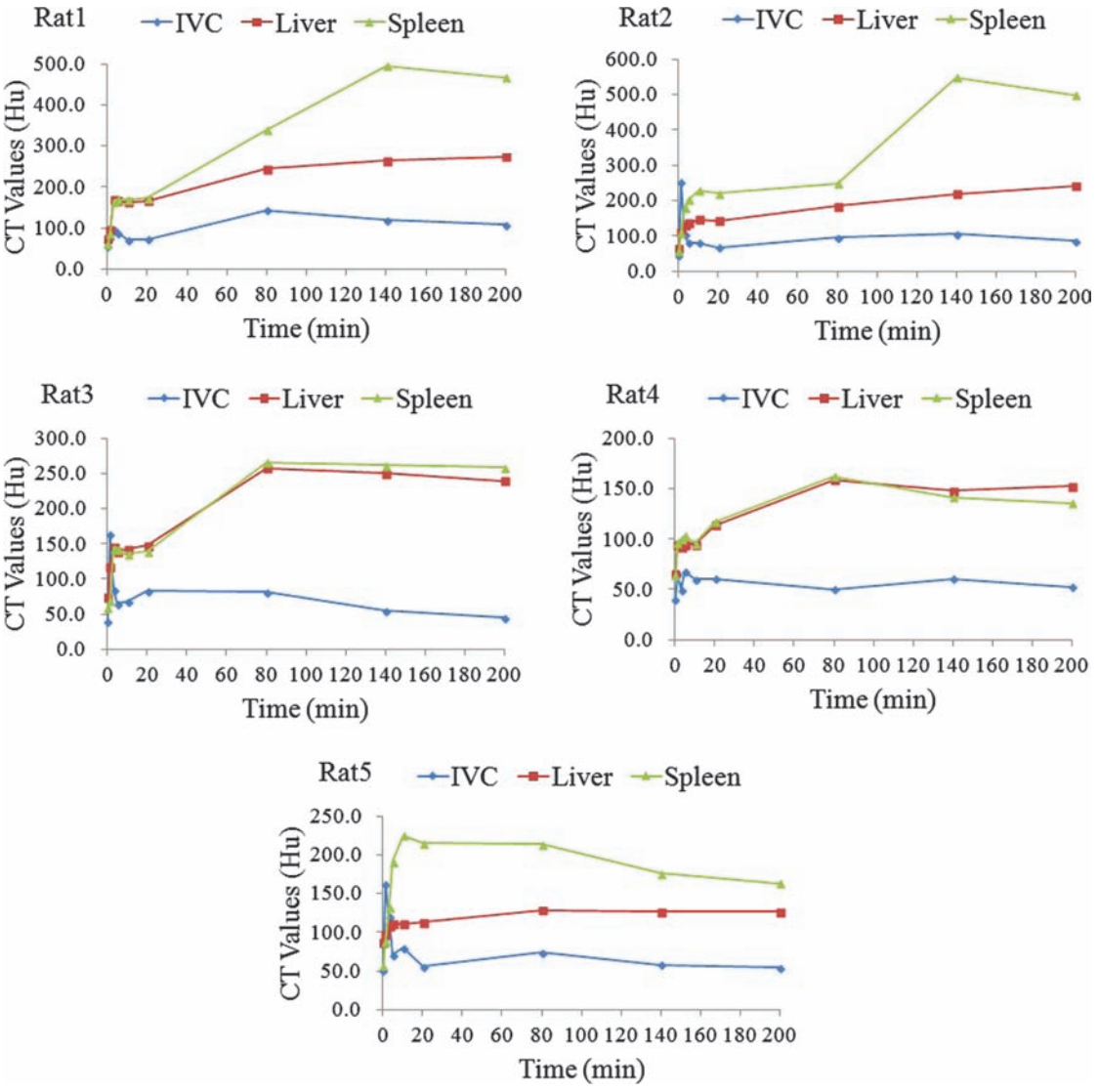

Figure 6. Plots of CT values of inferior vena cava, liver and spleen with time in the rat 1–5.

short stable stage after 5 min. The contrast agent gradually accumulated in the spleen. The CT values reached the top around 150 min in the rat 1 and 2, which appeared at around 80 min in the rat 3, 4 and 5.

The concentrations and dosages of the nanoemulsion injected into the rats 2, 3 and 5 were the same and the size of nanoemulsion injected into the rat 2 was largest (100 nm). The larger sized contrast agents had difficulty gathering in the liver and they instead preferred gathering in the spleen.

The changes of CT values in rat 1, 3 and 4 suggested that if the nanoemulsion was at the same concentration (48 mg · I/mL) and size (60 nm), the less dosage led to weaker CT efficacy and smaller CT values in the spleen. For example, when compared with the nanoemulsion in rat 1, same concentration and size with 40% dosage nanoemulsion was administrated into rat 4. The CT imaging in spleen suggested that only 30% of nanoemulsion accumulated in the spleen with earlier peak in rat 4.

3.4.4. In Vivo Metabolism

To analyze and discuss the influence of different sizes and dosage of nanoemulsion in the rat's metabolism, we comprehensively compared the CT values in the inferior vena cava, liver and spleen from each rat according to the Tables II–IV. From results shown in Figure 6, the concentrations in the inferior vena cava were significantly higher than in the liver and spleen at the first 1 min after the injection of nanoemulsion. The iodinated oil nanoemulsion gathered gradually in the liver and was metabolized into the blood. Some nanoemulsions, which accumulated in the spleen, were digested by the lymphocytes and macrophages and finally released into the blood. The CT values from the inferior vena cava were significantly decreased, while the CT values from the spleen and liver decreased with metabolism after the arterial phase, as a result. The digested iodinated oil emulsion returned to the blood, leading to the increase of CT values in the inferior vena cava again. For individual rats, the CT values from the spleen were highest, followed by those from the liver, while the CT values from the inferior vena cava were lowest. These results were precisely influenced by the injected dosage and species difference.

4. CONCLUSION

In this study, iodinated oil nanoemulsions with three different sizes; 25 nm, 60 nm and 100 nm, was successfully synthesized, all exhibiting good monodispersity. The iodinated oil nanoemulsions were developed as dual-modal contrast agents for both CT and fluorescent imaging to study the distribution and metabolism of these agents in the inferior vena cava, liver, and spleen from the rats, and also to compare their effect on the CT imaging of different organs according to their different sizes and doses. The results demonstrated that the target organs for the iodinated oil nanoemulsions were the livers and spleens, with obvious dosage-dependence. The larger sized nanoemulsion preferably accumulated in the spleen and liver, and its phagocytosis was weaker with the decrease of the nanoemulsion size. The CT imaging in the inferior vena cava was rapidly enhanced after administration of the nanoemulsion. The nanoemulsions gradually gathered and metabolized in the spleen and liver, rapidly decreasing the CT imaging in the inferior vena cava.

Conflict of Interests

The authors declare that there is no conflict of interests regarding the publication of this paper.

Acknowledgments: This work was supported by the National Natural Science Foundation of China (61072027 and 61127002).

References and Notes

1. J. Cheon and J.-H. Lee, *Acc. Chem. Res.* 41, 1630 (**2008**).
2. C. M. Gomes, A. J. Abrunhosa, P. Ramos, and E. K. Pauwels, *Adv. Drug Deliv. Rev.* 63, 547 (**2011**).
3. E. Orocio-Rodríguez, G. Ferro-Flores, C. L. Santos-Cuevas, F. D. M. Ramírez, B. E. Ocampo-García, E. Azorín-Vega, and F. M. Sánchez-García, *J. Nanosci. Nanotechnol.* 15, 4159 (**2015**).
4. R. T. Unni, G. A. Shah, K. Snima, C. R. Kamath, S. V. Nair, and V.-K. Lakshmanan, *J. Bionanosci.* 8, 101 (**2014**).
5. H. Hricak, *Pediatr. Radiol.* 41, 141 (**2011**).
6. R. Weissleder, *Science* 312, 1168 (**2006**).
7. H. R. Herschman, *Science* 302, 605 (**2003**).
8. J. M. Rosenholm, I. I. Vlasov, S. A. Burikov, T. A. Dolenko, and O. A. Shenderova, *J. Nanosci. Nanotechnol.* 15, 959 (**2015**).
9. J. M. Bryson, K. M. Fichter, W.-J. Chu, J.-H. Lee, J. Li, L. A. Madsen, P. M. McLendon, and T. M. Reineke, *Proc. Natl. Acad. Sci.* 106, 16913 (**2009**).
10. T. Atanasijevic, M. Shusteff, P. Fam, and A. Jasanoff, *Proc. Natl. Acad. Sci.* 103, 14707 (**2006**).
11. D. Simberg, T. Duza, J. H. Park, M. Essler, J. Pilch, L. Zhang, A. M. Derfus, M. Yang, R. M. Hoffman, and S. Bhatia, *Proc. Natl. Acad. Sci.* 104, 932 (**2007**).
12. B. Onel, C. Lin, and D. Yang, *Sci. China Chem.* 57, 1605 (**2014**).
13. M. A. A. Shah, N. He, Z. Li, Z. Ali, and L. Zhang, *J. Biomed. Nanotechnol.* 10, 2332 (**2015**).
14. R. T. Unni, G. A. Shah, K. Snima, C. R. Kamath, S. V. Nair, and V.-K. Lakshmanan, *J. Bionanosci.* 8, 101 (**2014**).
15. X. Ji, W. Yang, T. Wang, C. Mao, L. Guo, J. Xiao, and N. He, *J. Biomed. Nanotechnol.* 9, 1672 (**2013**).
16. X. Zhang, J. Zhu, F. Liu, Y. Li, A. Chandra, L. S. Levin, F. Beier, M. Enomoto-Iwamoto, and L. Qin, *Bone Res.* 2, 14015 (**2014**).
17. R. Huang, Z. Xi, and N. He, *Sci. China Chem.* 58, 1122 (**2015**).
18. C. Solans, P. Izquierdo, J. Nolla, N. Azemar, and M. Garcia-Celma, *Curr. Opin. Colloid In.* 10, 102 (**2005**).
19. L. Zhang, Z. Lu, Y. Bai, T. Wang, Z. Wang, J. Chen, Y. Ding, F. Yang, Z. Xiao, and S. Ju, *J. Mater. Chem. B* 1, 1289 (**2013**).
20. L. Song, F. Zang, M. Song, G. Chen, and Y. Zhang, *J. Nanosci. Nanotechnol.* 15, 4111 (**2015**).
21. L. Jin, X. Zeng, M. Liu, Y. Deng, and N. He, *Theranostics* 4, 240 (**2014**).
22. Z. Xi, R. Huang, Y. Deng, and N. He, *J. Biomed. Nanotechnol.* 10, 3043 (**2014**).

23. P. A. Jarzyna, T. Skajaa, A. Gianella, D. P. Cormode, D. D. Samber, S. D. Dickson, W. Chen, A. W. Griffioen, Z. A. Fayad, and W. J. Mulder, *Biomaterials* 30, 6947 **(2009)**.
24. A. Gianella, P. A. Jarzyna, V. Mani, S. Ramachandran, C. Calcagno, J. Tang, B. Kann, W. J. Dijk, V. L. Thijssen, and A. W. Griffioen, *ACS Nano* 5, 4422 **(2011)**.
25. Y.-H. Wang, L.-N. Song, J.-L. Ding, S.-S. Lu, Y.-N. Jiang, Y. Zhang, and N. Gu, *J. Southeast Univ.-Med.* 30, 671 **(2011)**.
26. W. Krause, *Adv. Drug Deliv. Rev.* 37, 159 **(1999)**.
27. W. H. Kong, W. J. Lee, Z. Y. Cui, K. H. Bae, T. G. Park, J. H. Kim, K. Park, and S. W. Seo, *Biomaterials* 28, 5555 **(2007)**.
28. K. E. DeKrafft, Z. Xie, G. Cao, S. Tran, L. Ma, O. Z. Zhou, and W. Lin, *Angew. Chem.* 121, 10085 **(2009)**.
29. S. Hou, L. Liang, S. Deng, J. Chen, Q. Huang, Y. Cheng, and C. Fan, *Sci. China Chem.* 57, 100 **(2014)**.
30. F. Song, H. Ning, H. She, J. Wang, and X. Peng, *Sci. China Chem.* 57, 1043 **(2014)**.
31. J. Fan, H. Yang, M. Liu, D. Wu, H. Jiang, X. Zeng, S. Elingarami, Z. Li, S. Li, and H. Liu, *J. Nanosci. Nanotechnol.* 15, 1123 **(2015)**.
32. F. Liu, D. Deng, X. Chen, Z. Qian, S. Achilefu, and Y. Gu, *Mol. Imag. Biol.* 12, 595 **(2010)**.

Received: 7 July 2015. Accepted: 23 October 2015.